ISSN: 3066-716X
Research Article
Journal of Clinical and Biomedical Advances

Preparation, Characterization, in Silico and in Vitro Antimicrobial Studies of Phenothiazine-3-Sulphonamide Derivatives

Eugene L. Ayuk[1], Magdalene O. Uchegbu[2*], Peace I. Ebiem-Kenechukwu[3], & Timothy O. Oni[4]

[1, 2]Department of Chemical Sciences, Godfrey Okoye University, Enugu-400001, Nigeria
[3]Material and Energy Technology Department, Projects Development Institute (PRODA), Enugu-400001, Nigeria
[4]Department of Science Laboratory Technology, Delta State Polytechnic, Ogwashi-Ukwu-320107, Nigeria

[*]Corresponding author: Magdalene O. Uchegbu, Department of Chemical Sciences, Godfrey Okoye University, Enugu-400001, Nigeria.

Submitted: 07 July 2025 **Accepted:** 14 July 2025 **Published:** 21 July 2025

https://doi.org/10.63620/MKJCBA.2025.1047

Citation: *Ayuk, E. L., Uchegbu, M. O., Ebiem-Kenechukwu, P. I., & Oni, T. O. (2025). Preparation, Characterization, in Silico and in Vitro Antimicrobial Studies of Phenothiazine-3-Sulphonamide Derivatives. J of Clin Bio Med Adv, 4(4), 01-12.*

Abstract

In low- and middle-income nations, where treatment failures and healthcare expenses are on the rise, the growing prevalence of antimicrobial resistance (AMR) presents a combined danger to world health and economic stability. FTIR, ^{1}H-NMR, and ^{13}C-NMR spectroscopy were used in this investigation to synthesize and characterize new phenothiazine-3-sulphonamide derivatives. Staphylococcus aureus (ATCC: 6538), Salmonella typhi (ATCC: 25175), Streptococcus pyogenes (ATCC: 27853), Escherichia coli (ATCC: 3008), and Aspergillus fumigatus (ATCC: 10231) are among the therapeutically relevant pathogens against which their antibacterial ability was evaluated using minimum inhibitory concentration (MIC) and in vitro agar well diffusion techniques. Furthermore, Auto Dock Vina's in silico molecular docking demonstrated significant binding affinities to microbial target proteins, with binding energies ranging from -5.1 to -7.6 kcal/mol. Antimicrobial activity of the synthesized compounds was on par with that of common medications like gentamycin, ketoconazole, and ciprofloxacin.

Keywords: Phenothiazine, Sulphonamide, Antimicrobial, In Silico, Drug Development, Public Health.

Introduction

Due to their wide range of pharmacological properties, phenothiazine derivatives have attracted a great deal of attention in the field of medicinal chemistry [1]. The phenothiazine molecule (Figure 1) is a tricyclic molecule made of two benzene rings joined to a heterocyclic ring containing nitrogen and a sulphur atom [2, 3]. Numerous biological activities, such as antibacterial, anticancer, antipsychotic, and antiinflammatory, have been reported in favor of these classes of compound and they have been widely used in the pharmaceutical industry as starting materials for drug molecules [4].

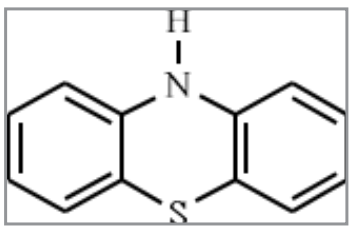

Figure 1: Phenothiazine Structure

Heinrich August Bernthsen, a German Chemist, produced phenothiazine for the first time in 1876 [5]. However, it wasn't until a few decades later that its prospective applications were looked into. Paul Charpentier and Henri Laborit led a research team at the French pharmaceutical company, Rhône- Poulenc, where they examined numerous substances for their antihistaminic qualities in the 1930s. They discovered that phenothiazine derivatives exhibited amazing antihistaminic properties [6]. During World War II, the antimalarial and antiparasitic effects of phenothiazine compounds were investigated, amongst these were promethazine 2 and chlorpromazine 3 (Figure 2) just to mention but a few and were discovered to possess good antimalarial properties.

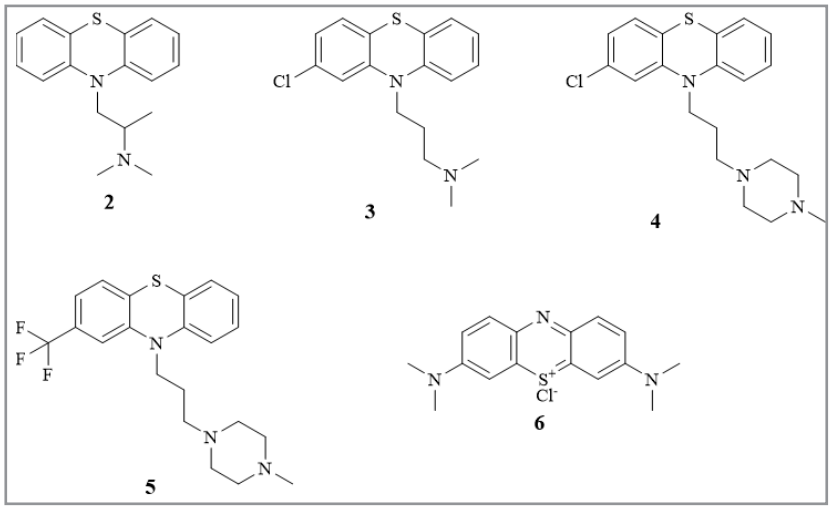

Figure 2: Chemical Structures of Some Phenothiazine Compounds

However, some of the derivatives were ineffective against the Plasmodium parasites, the causative agent of malaria but exhibited tranquilizing and relaxing effects, which raised curiosity about their possible psychiatric applications [7].

In the 1950s, the French researchers Jean Delay, Pierre Deniker and others discovered that phenothiazine compounds had potent antipsychotic properties [8]. Consequently, the first-generation antipsychotic medications were synthesized when it was discovered that chlorpromazine 3, originally produced as an antihistamine could also reduce psychotic symptoms [9]. These discoveries completely changed the view on the treatment of mental disorders, notably schizophrenia [10].

Further investigation on phenothiazine derivatives as therapeutic agents was sparked by the success of chlorpromazine 3 in psychiatry [11]. Over time, scientists synthesized a variety of phenothiazine compounds with unique pharmacological properties namely; prochlorperazine 4 (an antiemetic), promethazine 2 (an antihistamine and an antiemetic), trifluoperazine 5 (an antipsychotic), and methylene blue 6 (an antimalarial and a diagnostic agent). The discovery of phenothiazine and its derivatives brought a considerable impact on medicinal chemistry, especially in the treatment of psychiatric diseases, thereby clearing the pathway for the production of antipsychotic medications for the treatment of mental diseases [12].

Sulphonamide 7 is a general term for p- aminobenzenesulphonamide 8 derivatives which share some similarities with p-aminobenzoic acid (PABA) 9 (Figure 3). According to Lavanya, sulphonamides were among the first effective antibacterial medications used for treating bacterial infections in humans. Furthermore, sulphonamides have been used as diuretics, carbonic anhydrase inhibitors, and antibacterials [13, 14].

Nobel Prize winner Gerhard Domagk discovered prontosil and its antibacterial properties in the early 1900s. In an effort to keep Streptococci from harming his daughter, he discovered that the sulphonamide dye (prontosil) could selectively inhibit the infectious bacterium cells [15]. In 1936, Ernest Fourneau identified the protosil pathway in the human body by reporting that the dye was a prodrug (N-4 substituted sulphonamide) 10 (Figure 4) which metabolizes when ingested into sulphanilamide, 8, the active ingredient as an antibacterial in the human body.

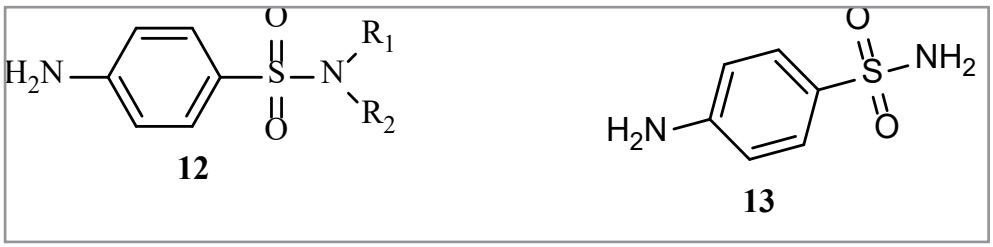

R1/R2 = H, alkyl, aryl or hetero aryl group

Figure 3: Structures of Sulphonamide, P-Aminobenzenesulphonamide and P-Aminobenzoic Acid

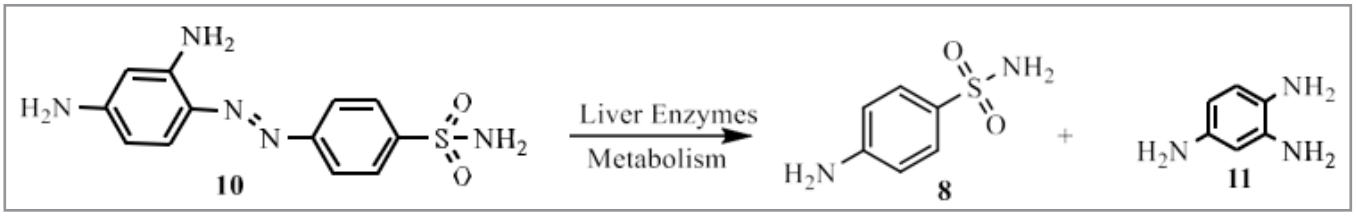

Figure 4: Metabolism of prontosil (a prodrug) to sulphonmaide (a metabolite form).

From 1950s till the present day, the synthesis of more potent high-profile sulpha drugs is still in progress. These include the antibacterial agent, sulphathiazole 12 [16], the carbonic anhydrase inhibitor, acetazolamide 13 [17][18] which has been in use clinically for more than 45 years, the diuretic agent, Furosemide 14 [19] the hypoglycemic agent glibenclamide 15 [20], the anti-cancer sulphonamide, indisulam 16 [21], the aspartic HIV protease inhibitor amprenavir 17 [22] used for AIDS and HIV infection management and the metalloprotease (MMP) inhibitors 18 of the sulphonyl amino acid hydroxamate [23] just to mention but a few (Figure 5).

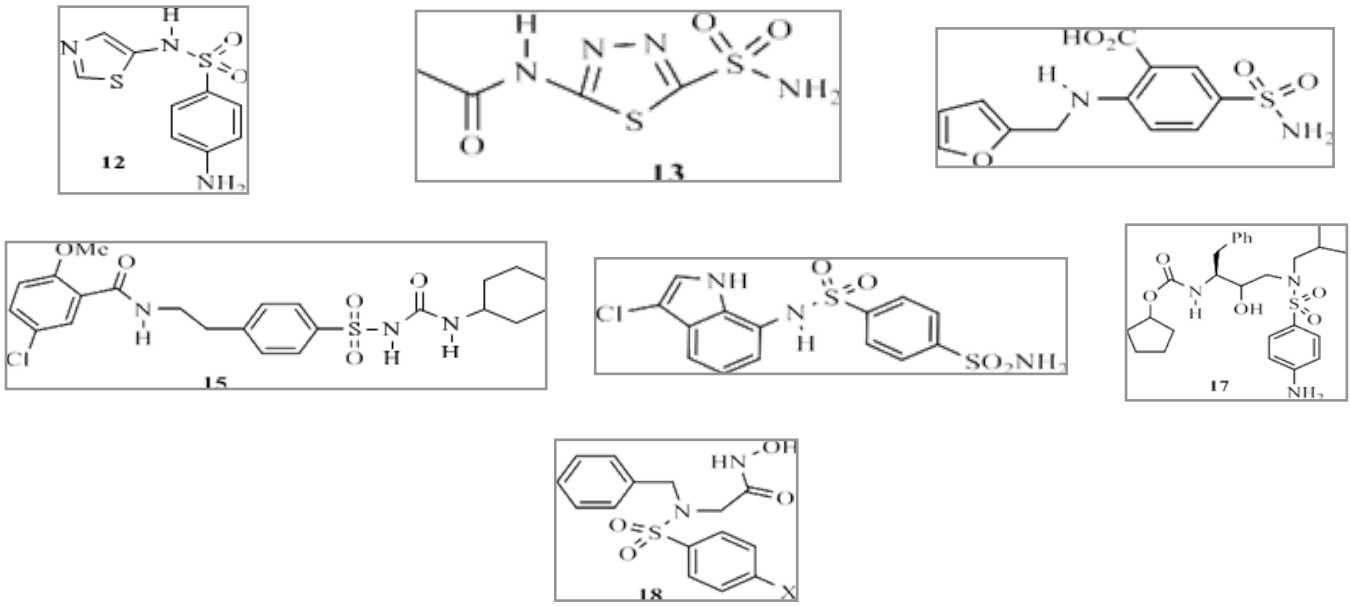

Figure 5: Chemical structures of some sulphonamide drugs.

Studies have shown that the presence of folate (folic acid) 22 is very vital in the manufacture of nucleic acids present in the cell wall of bacteria while its absence renders the cells inactive and prevents DNA synthesis. This can be seen when sulphonamide 8 reacts with dihydropteridine diphosphate 19 to form dihydropteroic sulphonamide 23 in the pathway B (Figure 6) which hinders further reaction for the formation of folic acid. This is because the formation of dihydropteroic acid 20 which proceeds to yield dihydrofolic acid 21 when dihydropteridine diphosphate 19 reacts with PABA 9 in part way A (Figure 6) cannot take place when sulphonamide is involved [21-25]. This clearly shows that sulponamide compounds exhibit bacteriostatic rather than bactericidal effects. These observations are illustrated in the scheme (Figure 6)

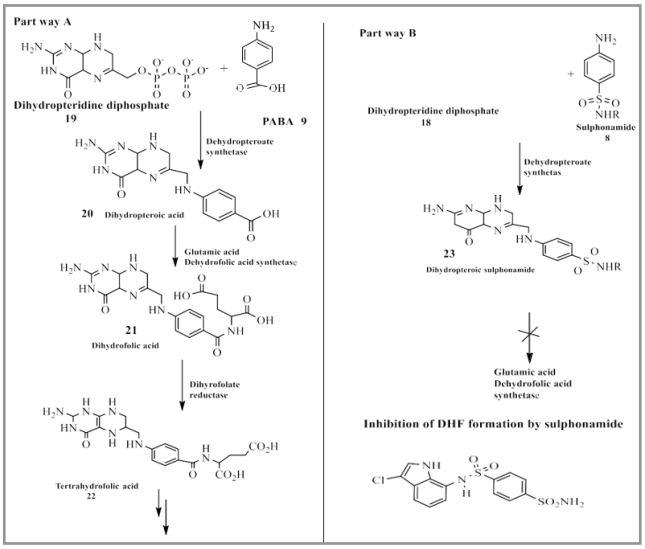

Figure 6: Reaction Pathway for Both Para-Aminobenzoic and Sulphonamide Molecules

Studies have also shown that sulphonamides and phenothiazine derivatives as individual single entities coupled with other moieties tend to exhibit tremendous pharmacological activities [26-30]. Supporting this claim, Kenia et al. reported that substitution of electron withdrawing group at position-2 of the phenothiazine ring increases antipsychotic activity. The effect of these groups on antipsychotic activity can be ranked as: R2 = SO2NR2 > CF3 > COCH3 > Cl, while substitution at position-3 can improve activity more than non- substituted compounds, but not significantly. Furthermore, the authors Kenia et al. also claimed that substituent at position-4 might hinder the receptor from binding to sulphur at position-5 due to steric hindrance. In addition to the above observations made by Kenia et al. they also maintained that the nature of substituent at position-10 also influences pharmacological activity. This observation explains why compounds with aliphatic side chain e.g. chlorpromazine 3 and triflupromazine 24 are less potent but clinically effective (Figure 7).

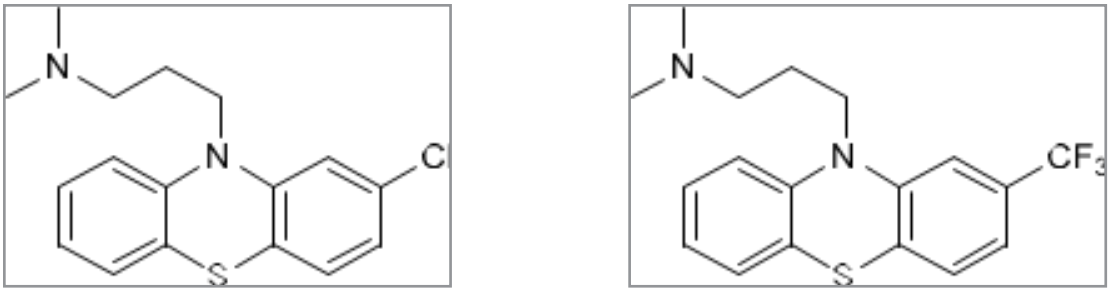

Figure 7: Structures of Chlorpromazine and Triflupromazine

These findings underscore the importance of substituted phenothiazines surrogates as targeted materials for drug synthesis. Therefore, since phenothiazines and sulphonamides derivatives exhibit pharmacological properties, it is our expectation that the coupling of these classes of compounds as a single molecule would yield a derivative with broad spectrum of pharmacological properties. Consequently, this expectation inspired the research work reported in this article [31-33].

Materials and Methods

Chemicals

All chemical reagents and solvents used were obtained from Aldrich, MolyChem, JHD and Burgoyne, and used without purification. Joel 400MHz spectrometers in CDCl3 using TMS as internal standards were used in recording 1H-NMR and 13C-NMR spectra. FTIR spectra of the compounds were run in PerkinElmer Spectrum version 10.03.06 and the bands represented in wave number. Melting points were determined in open capillary tubes and were uncorrected. All experiments were carried out at the Chemistry Laboratory, Department of Chemical Sciences, Godfrey Okoye University, Thinkers Corner in Enugu, Enugu State. Computational Tools: ChemDraw (used specifically in drawing chemical structures and molecular modeling), protein-ligand design and virtual screening (BIOVIA discovery Studio); used in analyzing protein and ligand structures, performing structural alignment, identifying binding sites, and analyzing protein- ligand interactions, molecular docking software (AutoDock Vina); used in predicting the binding affinities and interactions of the synthesized derivatives with target proteins, molecular modeling and visualization software (PyMOL); used for analyzing and visualizing molecular structures and interactions.

Methods

Synthesis of 1-(Naphthalen-1-yl)Benzene-1,4-Diamine (27)

A mixture of 1-naphthylamine 25 (2.0 mmol) and 4-chloroaniline 26 (2.0 mmol) in dimethyl formamide (25 mL) was refluxed in the presence of anhydrous potassium hydroxide (2.0 mmol) for 3 h using an oil bath. The mixture was filtered and the residue was washed with 10.0 mL hot dimethylformamide. The filtrate obtained was poured into ice cold water, followed by acidification with 10.0 mL dilute HCl. The precipitate was washed twice with dichloromethane (30 ml) and finally with ethylacetate (3×20 mL) in a separating funnel. The organic layers obtained were combined and air dried to give a colored solid product, 1-(naphthalen-1-yl)benzene-1,4-diamine 27.

Yield 75.7%, melting point 190–191 °C. FTIR (KBr, cm-1): 3350.9 (N–H stretch), 3049 (C–H aromatic), 1617 (C=C aromatics), 1285 (C–N). 1H NMR (δ): 8.85 (s, 1 H, NH proton), 8.22 (s, 1 H, ArH), 8.15 (s, 1 H, ArH), 7.73 (t, 3 H, J = 0.8 Hz, ArH), 7.71 (d, 2 H, J = 8.0 Hz, ArH), 7.34 (d, 2 H, J = 0.4 Hz, ArH), 6.21 (s, 2 H, ArH), 4.95 (d, 2 H, J = 3.0 Hz, NH2). 13C NMR (δ): 142.7 (1C), 135.9 (1C), 130.3 (1C), 130.0 (1C), 127.8 (1C), 127.3 (1C), 126.8 (1C), 126.4 (1C), 125.8 (1C), 125.6 (1C), 123.4 (1C), 122.5 (1C), 120.5 (1C), 118.5 (1C). HRMS-ESI (m/z) for C16H14N2: 230.10 [M]+, calculated 234.30.

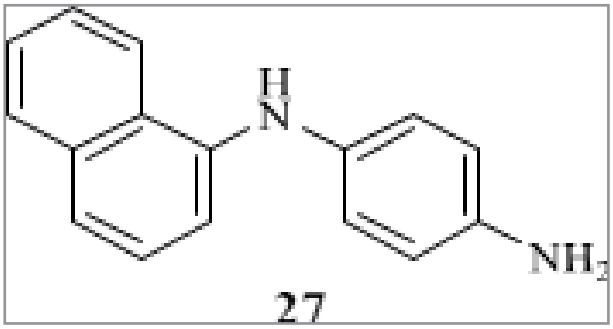

Figure 8: 1-(Naphthalen-1-yl)Benzene-1,4-Diamine (27) Structure.

Synthesis of 12H-Benzo[a]Phenothiazin-9-Amine (28)

A mixture of 1-(naphthalen-1-yl)benzene-1,4- diamine 27 (0.4 mmol), sulphur powder (0.8 mmol) and a iodine crystals (0.8 mmol) in 1,2- dichlorobenzene (20 mL) was refluxed for 5 h in oil bath. The reaction mixture was then distilled to remove excess solvent. The product obtained was then recrystallized from acetone, filtered and allowed to air dry and a dark colored solid product was obtained. Yield 83.4%, m.p. 250 °C. FTIR (KBr, cm-1): 3388 (N–H stretch), 3049 (C–H aromatic), 1617 (C=C aromatics), 1248 (C–N). 1HNMR (δ) 8.21 (d, 1 H, NH), 7.82 (s, 1 H, ArH), 7.73–7.71 (t, 3 H, J = 0.8 Hz, ArH), 7.65 (s, 1 H, ArH), 7.52–7.54 (m, J = 0.8 Hz, 2 H, ArH), 7.34–7.32 (d, J = 0.8 Hz, 2 H, ArH), 4.89 (s, 2 H, NH2). 13C NMR (δ): 152 (1C), 142.7 (1C), 135.9 (1C), 130.3 (1C), 130.0 (1C), 127.8 (1C), 127.3 (1C), 126.8 (1C), 126.4 (1C), 125.8 (1C), 125.6 (1C), 123.4 (1C), 122.5 (1C), 120.5 (1C), 118.5 (1C), 111.5 (1C) (16 aromatic carbons). HRMS-ESI (m/z) for Chemical Formula: C16H12N2S: 263.24 [M+H]+, calculated 264.35.

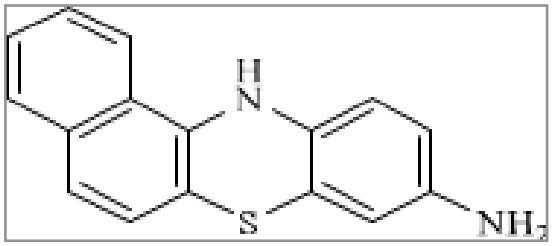

Figure 9: 12H-Benzo[a]Phenothiazin-9-Amine Structure

General Method for the Synthesis of Phenothiazine-3-Sulphonamides Derivatives (30a-c)

Sodium carbonate, Na2CO3 (0.5 mmol) was weighed and added to a solution of 12H-benzo[a] phenothiazin-9-amine 28 (0.1 mmol) in dichloromethane (20 mL) and acetone with continuous stirring using a magnetic stirrer until all the solutes were dissolved. The appropriate substituted arylsulphonyl chlorides 29 a-c (1.0 mmol) were added in three portions over a period of 45 minutes. The solution was refluxed for 10 h in water bath. After completion, the pH of the reaction mixture was adjusted from 7 to 2 using 2 M HCl (5 mL) and a cloudy solution was obtained. The organic portion was extracted with dichloromethane (50 mL) and ethylacetate (50 mL), and left to air- dry [34, 35].

N-(12H-Benzo[a]Phenothiazine-9-yl)-4- Methylbenzenesulphonamide (30a)

Yield 82.5%, melting point 240–241 °C. FT-IR (KBr, cm-1) 3369 (N–H stretch), 3063 (C–H aromatic), 2914 (C–H stretch), 1625 (C=C aromatics), 1375 (S=O vibration of sulphonamide), 1319.5 (C–N). 1H NMR (δ): 9.60 (s, 1 H, NH), 8.15 (s, 1 H, SO2NH of amide), 7.81 (s, 1 H, ArH), 7.79 (s, 1 H, ArH), 7.50–7.61 (m, 7 H, J=4.4 Hz, ArH), 7.59 (d, 2 H, J=0.8Hz, ArH), 7.15 (s, 1 H, ArH), 6.97 (s, 1 H, ArH), 2.40 (s, 1 H, ArCH3). 13C NMR (δ): 144.6 (1C) 142.7 (1C), 135.9 (1C), 130.3 (1C), 130.0 (1C), 127.8 (1C), 127.3 (1C), 126.8 (1C), 126.4 (1C), 125.8 (1C), 125.6 (1C), 123.4 (1C), 122.5 (1C), 120.5 (1C), 118.5 (1C), 111.6 (1C), 111.5 (1C). HRMS-ESI (m/z) for C23H18N2O2S2: 420.01 [M-2H]+, calculated 418.53.

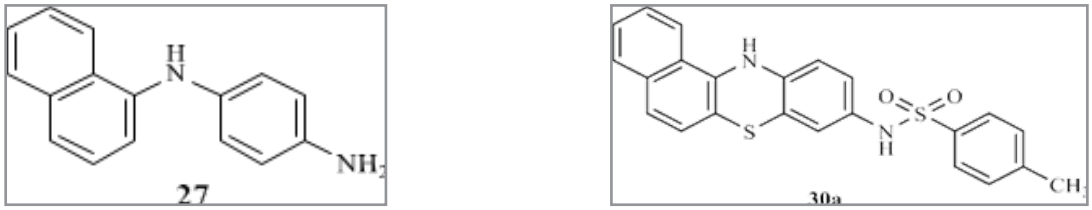

Figure 10: N-(12H-Benzo[a]Phenothiazine-9-yl)-4- Methylbenzenesulphonamide Structure.

N-(12H-Benzo[a]Phenothiazine-9-yl) Benzenesulphonamide (30b)

Yield 80.6%, melting point 195–196 °C. FTIR (KBr, cm-1): 3350 (N–H stretch), 3063 (C–H aromatic), 2922 (C–H stretch), 1621 (C=C aromatics), 1379 (S=O vibration of sulphonamide), 1330 (C–N). 1H NMR (δ): 9.60 (s, 1 H, NH), 8.15 (s, 1 H, SO2NH of amide), 7.85 (s, 1 H, ArH), 7.75 (t, 3 H, J = 0.4 Hz, ArH), 7.55–7.57 (m, 4 H, J = 0.8 Hz, ArH), 7.49 (d, 2H, J = 0.2, Hz, ArH), 7.15 (s, 1H, ArH), 6.87 (s, 1H, ArH), 6.61 (s, 1 H, ArH), 6.23 (s, 1H, ArH). 13C NMR (δ): 144.6 (1C), 143.1 (1C), 142.7 (1C), 135.9 (1C), 132.2 (1C), 130.3 (1C), 130.0 (1C), 128.3 (1C), 127.8 (1C), 127.3 (1C), 126.8 (1C), 126.4 (1C), 125.8 (1C), 125.6 (1C), 123.4 (1C), 122.5 (1C), 120.5 (1C), 118.5 (1C), 118.0 (1C), 111.6 (1C), 111.5 (1C). HRMS-ESI (m/z) for C22H16N2O2S2: 406.11 [M-2H]+, calculated 404.16.

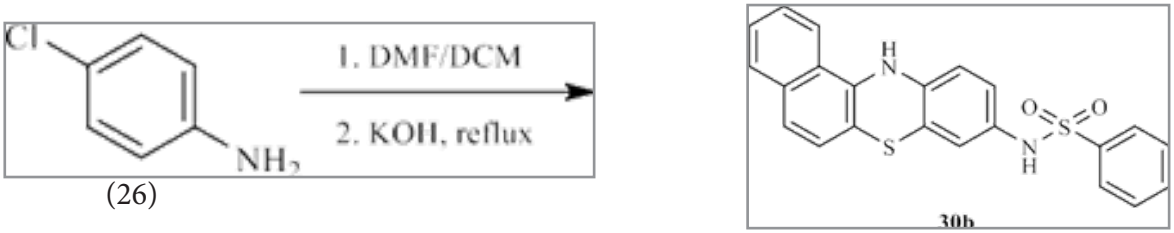

Figure 11: N-(12H-benzo[a]phenothiazine-9-yl) benzenesulphonamide structure.

N-(12H-benzo[a]phenothiazine-9-yl)-4-nitrobenzenesulphonamide (30c)

Yield 81.9%, melting point 237–238 °C. FTIR (KBr, cm-1): 3388 (N–H stretch), 2079 (C–H aromatic), 1625 (C=C aromatics), 1524 (N–O stretch), 1360 (S=O vibration of sulphonamide), 1211 (C–N). 1H NMR (δ): 9.80 (s, 1 H, NH), 8.37– 8.35 (d, 2 H, J=0.8 Hz, SO2NH of amide), 8.21 (s, 1H, ArNO2), 8.01 (d, 1 H, ArH), 7.85 (s, 1 H, ArH), 7.78 (s, 1 H, ArH), 7.64 (s, 1 H, ArH), 7.45–7.44 (d, 2 H, J = 0.4 Hz, ArH), 6.80 (s, 1 H, ArH), 6.75 (s, 1H, ArH), 6.69 (s, 1 H, ArH), 6.60 (s, 1 H, ArH). 13C NMR (δ): 152.5, (1C), 144.6 (1C), 143.1, (1C), 142.7 (1C), 135.9 (1C), 132.2 (1C), 130.3 (1C), 130.0 (1C), 128.3 (1C), 127.8 (1C), 127.3 (1C), 126.8 (1C), 126.4 (1C), 125.8 (1C), 125.6 (1C), 123.4 (1C), 122.5 (1C), 120.5 (1C), 118.5 (1C), 118.0 (1C), 111.6 (1C), 111.5 (1C). HRMS- ESI (m/z) for C22H15N3O4S2: 447.17 [M+2H]+, calculated 449.50.

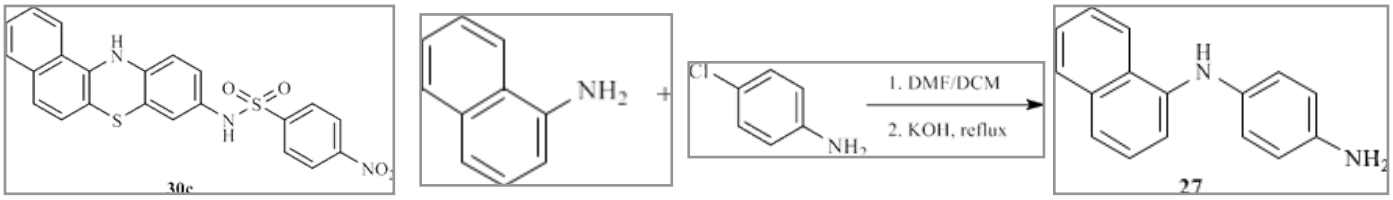

Figure 12: N-(12H-benzo[a]phenothiazine-9-yl)-4-nitrobenzenesulphonamide structure

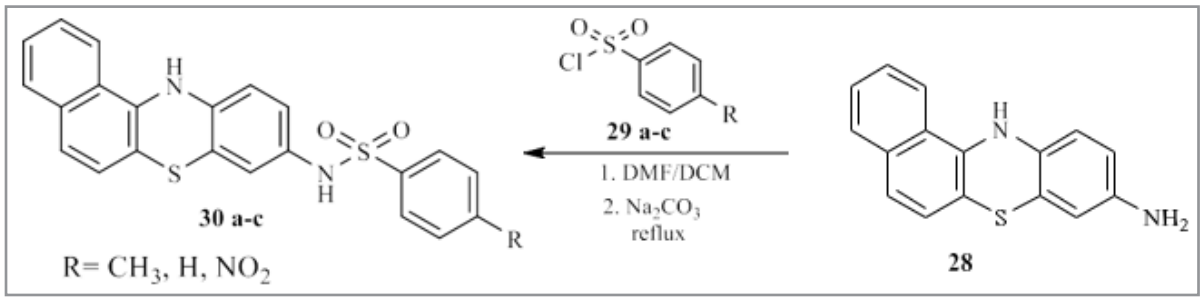

Figure 13: Synthesis of Substituted Phenothiazine-3-Sulphonamide Derivatives

Biological Studies

The antimicrobial activity of the synthesized phenothiazine-3-sulphonamide derivatives against clinical pathogens was determined via agar well diffusion method based on the guidelines given by the National Committee for Clinical Laboratory Standards NCCLS (2002) [36].

Preparation of Selected Derivatives Concentrations

The synthesized compounds, 12H-benzo[a]phenothiazin-9-amine 28, N-(12H-benzo[a] phenothiazine-9-yl)-4-methylbenzenesulponamide 30a, N-(12H-benzo[a]phenothiazine-9-yl) benzenesulphonamide 30b, and N-(12H-benzo [a] phenothiazine-9-yl)-4 nitrobenzenesulphonamide 30c were prepared in four different molar concentrations respectively. A stock solution was first prepared for each of the derivatives containing 5 mg/mL and the volume was made up by adding acetone (10 mL) to give the stock solution of each of the synthesized compounds. From the stock solution, different concentrations of the solutions of the compounds were prepared via serial dilution, thus: 2.5, 1.25, and 0.625 mg/mL [37].

Nutrient Agar Preparation

28.0 g of nutrient agar powder was suspended in a conical flask containing distilled water (1000 mL), mixed and dissolved completely. The flask and its content were sterilized by autoclaving at 121° C for 15 min, cooled at 37 °C and mixed thoroughly. The molten agar was then poured into the sterilized petri dishes and allowed to solidify [38].

The Test Microorganisms Used

Four human pathogenic bacteria made up of two Gram-positive Staphylococcus aureus (S. aureus) and Streptococcus pyogenes (S. pyogenes) and two Gram-negative Escherichia coli (E. coli) and Salmonella typhi (S. typhi) were used for the antibacterial assay while one fungus Aspergillus fumigatus (A. fumigatus) was used for the antifungal assay. All the organisms were local isolates from the Laboratory bacterial and fungi stock of Lifechart Medical Diagnostic Center, Enugu State, Nigeria and streaked unto already prepared nutrient agar [39].

Control Test (Standard)

The standard antibiotics used were ciprofloxacin and gentamycin, while ketoconazole was used as the antifungal drug.

Determination of Antimicrobial Activity

Sterile Mueller-Hinton agar plates were prepared for bacterial strains and sterile nutrient agar was prepared for fungal strain inoculated by a spread plate method under aseptic condition [40].

Preparation of Nutrient Agar for Fungal Strain

28.0 g of nutrient agar powder was suspended in distilled water (1000 mL). It was then mixed and dissolved completely, sterilized by autoclaving at 121 °C for 15 min. After autoclaving and allowing to cool down, 10 mg/mL of the antibiotic ciprofloxacin, was added. This was to stop bacteria inhibition [41].

Preparation of Mueller-Hinton Agar for Bacterial Strains

Mueller-Hinton agar (10.0 g) was dissolved in distilled water (300 mL) and dissolved completely. Sterilized by autoclaving at 121 °C for 15 min, the liquid was then poured into sixteen (16) petri dishes and allowed to solidify. After solidification, four wells of about 6 mm diameter were punched in each agar plates using a sterile gel puncher. The nutrient agar grown pathogenic cultures were then streaked on each agar plates using a sterile

wire loop, trying as much as possible to avoid the wells while streaking the entire plates [42]. About 100 µL of the different concentrations of 12H-benzo[a] phenothiazin-9-amine 28 and its sulphonamide derivatives (30a-c) were added into the wells using sterile micropipettes. The culture plates were incubated in inverted position at 37 °C for 24 h. Positive control was set using standard antibiotics (ciprofloxacin and gentamycin) and antifungal drug (ketoconazole) while a negative control was the solvent (acetone).

Determination of Minimum Inhibition Concentration (MIC)

12H-benzo[a]phenothiazin-9-amine 28 and its sulphonamide derivatives (30a-c) were used in the MIC determination via well diffusion method. The inoculum of microorganisms was prepared from nutrient agar cultures. In this method, the agar dilution technique of the samples were prepared to the highest concentration of 5 mg/mL (stock concentration) in acetone and serially diluted to working concentrations range 5 to 0.625 mg/mL using Mueller-Hinton Agar and later inoculated with 1 mL suspension of the test organisms [43]. The positive control was nutrient agar with standard reference antibiotics (gentamycin and ciproflaxin) and antifungal (ketoconazole) and inoculums. After 24 h of incubation at 37 °C, the samples were observed.

Molecular Docking Studies

Molecular docking was performed to predict the binding abilities of the synthesized compounds and the standard drugs; ciprofloxacin and gentamycin (antibacterial), ketoconazole (an antifungal) on the active sites of the receptors (proteins) of S. aureus, S. pyogenes, E. coli, S. typhi, and A. fumigatus, using AutoDock tools. Their 3D crystal structures of the respective microorganisms were downloaded from protein data bank as follows; PDB: 5YH5 with 2.90 Å resolution, PDB: 5YHP with 3.02 Å resolution, PDB: 6KZV with 2.40 Å resolution, PDB: 4W4M with 3.20 Å resolution, PDB: 5ZVP with 1.42 Å resolution, PDB: 2XCT with 3.35 Å resolution, and PDB: 2V0M with 2.80Å resolution [44]. ChemDraw Professional 15.0 was used for drawing the structures of the different derivatives. BIOVIA Discovery Studio 2017 R2 was then used for the preparation of the different proteins downloaded from the Protein Data Bank. Lastly, the PyRx app was used to perform the docking of the synthesized compound and the prepared proteins [44].

Physicochemical and Drug Likeness Properties Determination of Synthesized Compounds

For the calculation of the physicochemical and drug likeness properties of the synthesized compounds, the Swiss assessment of absorption, distribution, metabolism and excretion SwissADME web service and methodologies, a web tool for evaluating pharmacokinetics, drug- likeness of small molecules was used Antoine et al., developed and maintained by the Molecular Modeling Group of the Swiss Institute of Bioinformatics (SIB). The drug likeness properties of the synthesized compounds that were determined in this work include; MW-molecular weight, TPSA -topological polar surface area, HBA-hydrogen bond acceptor, HBD-hydrogen bond donator, Nrotb-number of rotable bonds, Nviolations- number of violations and LogP-lipophilicity. According to Lipinski et al. 'the rule of 5' (RO5) predicts that poor absorption or permeation is more likely when there are more than 5 H-bond donors, 10 H-bond acceptors, the molecular weight (MWT) is greater than 500 and the calculated Log P (CLogP) is greater than 5 (or MlogP > 4.15) for a given drug molecule [45].

Results and Discussions

The base catalyzed reaction of 1-naphthylamine 25 and 4-chloroaniline 26 in the presence of dimethylformamide yielded 1-(naphthalen-1-yl) benzene-1,4-diamine 27 one of the key intermediates as shown in Fig. 13. The FTIR spectrum of this compound gave absorption bands at 3350 cm-1 for NH stretch, 3049 cm-1 for C–H aromatic, 1617 cm-1 for C=C aromatic, and 1285 for C–N bending vibration. In the 1H-NMR spectrum, the peak at 8.85 ppm appeared as a singlet and was attributed to NH proton, the peaks at 7.71–6.21 ppm were attributed to the aromatic protons while the peak at 4.95 ppm was for two protons for NH2 of aniline ring. The 13C-NMR spectrum showed peaks 142.7–118.5 ppm for aromatic carbons. In order to obtain the phenothiazine derivative 28 1-(naphthalen-1-yl)benzene-1,4-diamine 27 was treated with sulphur powder and a catalytic amount of iodine crystals in 1,2-dichlorobenzene to furnish the product, 1-(naphthalen-1-yl)benzene-1,4- diamine and 12H-benzo[a]phenothiazin-9-amine 28 as shown in Figure 13 whose FTIR spectrum revealed bands at the following regions 3388 cm-1 for NH stretch, 3049 cm-1 for C-H aromatic, 1617 cm-1 for C=C aromatic, and 1300 cm-1 for C–N. In the 1H-NMR spectrum, there was a single peak at 8.21 ppm due to NH proton, at 7.82–7.71 for all the aromatic protons and a singlet at 4.89 ppm for two NH2 protons. The 13C-NMR spectrum showed peaks 152.1–111.5 ppm which were all assigned to aromatic carbons. The substituted phenothiazine-3- sulphonamide (30 a-c) derivatives were synthesized via base catalyzed reactions of 12H-benzo[a] phenolthiazin-9-amine and three substituted arylsulphonyl chlorides to yield the final products, phenothiazine-3-sulphonamide derivatives as shown in Figure 13. The structures of these derivatives were supported by spectral data. In the FTIR spectrum, the compounds show almost similar absorption band at 3350 cm-1 (NH stretch), 3063 cm-1 (aromatic C–H stretch), 2922 cm-1 (aliphatic C–H stretch), 1621 cm-1 (C=C aromatic), 1379 cm-1 (S=O vibration) and 1330 cm-1 was due to C–N bending. The 1H NMR spectra showed peaks at the expected regions for NH at 9.8–9.6 and 8.37–8.35 ppm for SO2-NH, at 7.85–6.61 ppm for aromatic protons while the 13C-NMR spectra of the compounds revealed peaks at 144.6–111.6 ppm assigned to aromatic carbons and at 19.9 ppm to methyl aliphatic carbon.

In Silico Antimicrobial Studies

The docking antimicrobial studies were conducted to predict the biological activities of both intermediates 27 and 28 as well the final product (30 a-c) on the microorganisms using their binding energies as presented in Table 1. Higher negative values of the binding energies suggest good activities of the compounds against the tested microorganisms [46]. The results on Table 1, showed compounds 30 b and 30 c exhibited higher binding energy values of 7.1 kcal/mol each for S. typhi comparable with the standard drugs ciprofloxacin and gentamycin with values of -7.4 and 7.0 kcal/mol, respectively. For S. aureus the intermediate 28 gave the highest binding energy value of -7.3 kcal/mol, comparable with the standard drugs ciprofloxacin and gentamycin with values of -7.6 and 7.0 kcal/mol. For E. coli, the higher binding energy value of -7.20 and -7.0 kcal/ mol was obtained for both compounds 30 a and 30 b as well as for 30 c (Figure 14) while for

S. pyogenes, the highest value of -7.4 kcal/mol was recorded for intermediate 28 when compared with comparable with the standard drugs. For the fungus A. fumigatus, compound 30 b gave the highest binding energy value of -7.5 kcal/mol comparable to the standard drug ketoconazole. The results obtained from in silico antimicrobial studies of the above compounds suggested that the phenothiazine and phenothiazine-3-sulphonamide compounds possessed good biological activities comparable with the standard drugs used for the investigation [47].

Table 1: Binding Energies (kcal/mol) for Antimicrobial in Silico Studies

Compounds	S. aureus	S. pyogenes	E. coli	S. typhi	A. fumigatus
27	-5.1	-5.3	-6.3	-5.7	-6.4
28	-7.3	-7.4	-6.3	-6.1	-7.1
30 a	-5.5	-5.7	-7.2	-6.3	-7.1
30 b	-5.9	-6.1	-7.2	-7.1	-7.5
30 c	-6.6	-6.6	-7.0	-7.1	-7.4
Ciprofloxacin	-7.6	-7.0	-6.1	-7.4	-
Gentamycin	-7.0	-7.3	-5.7	-7.0	-
Ketoconazole	-	-	-	-	-7.6

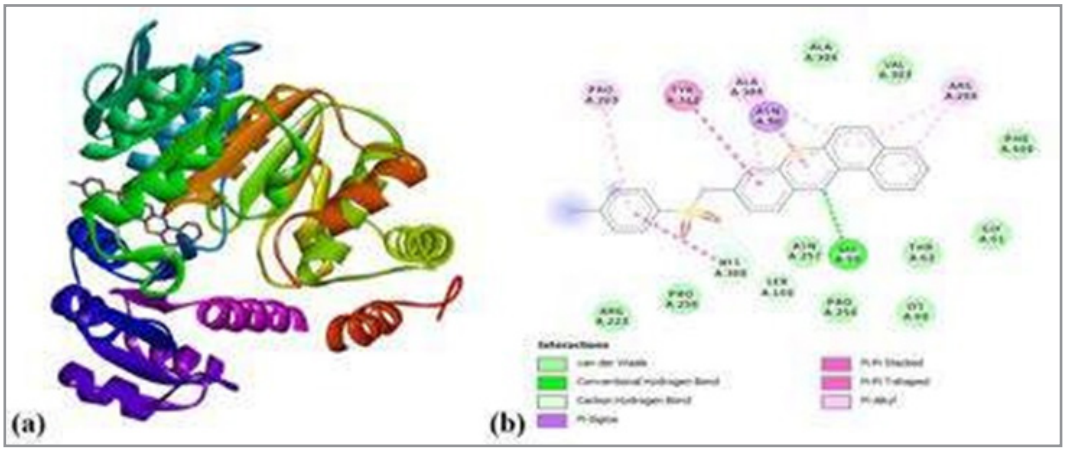

Figure 14: (a) 3D structure of 30 c bound to E. coli (b) 2D diagram displaying the hydrogen bonding and other interactions between 30 c and the amino acids residues in the active site.

These results agree with the experimental results presented in Table 3 and will provide more insight into the mechanism of inhibition for the synthesized compounds [48].

Comparative Estimation of The Physiochemical and Drug Likeness Properties of The Synthesized Compounds

The parameters that indicated the drug likeness of the prepared compounds according to Lipinski, (2004) include; MW-molecular weight, TPSA- topological polar surface area, HBA-hydrogen bond acceptor, HBD-hydrogen bond donator, Nrotb- number of rotable bonds, Nviolations-number of violations, miLogP-modified molecular hydrophobicity potential. Table 2 presents a summary of drug likeness properties of the prepared compounds.

Table 2: Physiochemical or Drug Likeness Properties of Synthesized Compounds

Compounds	MW*	miLogP	LogS	TPSA	HBA	HBD	Nviolations	Nrotb
28	264.07	4.22	-4.63	41.81	1	3	0	0
30a	418.08	6.36	-7.11	61.96	3	2	1	3
30b	404.07	5.73	-7.18	61.96	3	2	1	3
30c	449.05	5.91	-5.20	107.78	5	2	1	4
Acceptable threshold	<500 Da	<5	0 – (-6)	≤140 A2	≤10	≤5	0	9

An effective drug candidate should have a MW threshold of less than 500 g/mol based on Lipinski's RO5. Studies have proven the relationship between a drug's molecular weight (MW) and toxicity, suggesting that compounds with lower MW have reduced toxicity. For this reason, a benchmark of 500 g/mol has been established. Therefore, it is preferable to have low molecular weights. From the above table above, the four compounds obeyed Lipinski's RO5 of MW threshold, therefore needless for

optimization. According to Chapman et al., LogP is a measure of a chemical's hydrophobicity and is universally defined as the negative of the logarithm of the partition coefficient between n-octanol and water (Coctanol/Cwater). Consequently, an increase in LogP signals a decline in aqueous solubility, which lowers absorption. From the above table above, only compound 28 obeyed Lipinski's RO5 of LogP threshold while compounds 30a, 30b and 30c did not which suggests the need for structural optimization.

LogS determines the oral bioavailability of drugs in line with membrane permeability [49].The estimation is crucial because it influences the bioavailability of drugs based on membrane permeability. A look at the table above revealed that compounds 30a and 30b did not fall within the acceptable threshold range for LogS which suggest the need for structural optimization also. TPSA parameter totals the polar atoms at the surface which are primarily oxygen and nitrogen in addition to the hydrogen atoms that are attached to them. This parameter predicts the cell penetration ability of chemical compounds. Accordingly, it is said that the lower the TPSA value, the better. Substances with TPSA values less than 140 Å2 are more likely to cross the blood-brain barrier than those with TPSA values larger than 140 Å2. As a result, it is hypothesized that an increase in TPSA will reduce the ability of drugs to be transported, which will impact their biological activities. A look at the Table 2 suggests that compounds 28-30c did fall within the acceptable threshold range for TPSA, therefore needless for optimization [50].

The terms used to describe the hydrogen bonds that exist in a molecule are hydrogen bond donors (HBD) and acceptors (HBA). These parameters have been utilized frequently in the analysis of the drug likeness of compounds. According to Lipinski's RO5, a drug must have an HBD count of ≤5 and a HBA of ≤10 in order to be orally active [51]. A look at the table suggests that compound 28-30c did fall within the acceptable threshold range for HBA and HBD, therefore needless for optimization [52].

In Vitro Studies

The studies were conducted to determine the effects of the prepared compounds on the following microorganisms (S. aureus (ATCC: 6538) and S. pyogenes (ATCC: 27853), two Gram-negative bacteria; (E. coli (ATCC: 3008), and S. typhi (ATCC: 25175) as well as one fungus (A. fumigatus (ATCC: 10231) [32]. The lower the value of MIC, the better the activity of the compound. The results are presented in Table 3. Compound 30c exhibited the lowest MIC values for the first three bacterial strains and the fungus A. fumigatus comparable to the standard drugs. Compound 28 showed no result (NR) for E. coli. Compounds 28-30c showed no result (NR) for S. pyogenes, while compounds 28-30b showed no result (NR) for A. fumigatus. These observations call for further investigation on the activities of the compounds on these microorganisms by increasing the concentrations of the compounds.

Table 3: Minimum Inhibitory Concentrations of the Synthesized Compounds (mg/mL)

Compounds	S. aureus	S. pyogenes	E. coli	S. typhi	A. fumigatus
28	1.0	NR	NR	NR	NR
30 a	1.0	NR	2.0	1.5	NR
30 b	0.5	NR	3.5	2.0	NR
30 c	0.1	NR	0.5	1.0	0.5
Ciprofloxacin	0.5	0.5	0.5	0.5	NR
Gentamycin	0.5	0.5	0.5	0.5	NR
Ketoconazole	NR	NR	NR	NR	0.5
Note: NR: Not result					

Conclusions

The synthesis of 12H-benzo[a]phenothiazin-9- amine and three of its derivatives, phenothiazine-3- sulphonamides was successfully carried out. The FTIR, 1H-NMR, and 13C-NMR spectral data of all the synthesized compounds were consistent with the assigned structures. The in-silico studies revealed that the synthesized compounds exhibited different binding affinities against the different microorganisms. Compounds 30a and 30b showed higher binding energy of -7.2 kcal/mol for E. coli comparable with the standard drugs (ciprofloxacin and gentamycin) whose binding energies were -6.1 and -5.7 kcal/mol respectively. For S. pyogenes, compound 30 had a higher binding energy of -7.4 kcal/mol. This suggests that the compounds possess promising antimicrobial properties. Compounds 30a-c were also subjected to in vitro antimicrobial test and compound 30b exhibited the lowest MIC values (0.5–1.0 mg/mL) for all the tested microorganisms comparable to the standard drugs. This study has shown that phenothiazine derivative coupled with arysulphonyl chloride functionalities to form phenothiazine-3-sulphonamides as single conjugates possess promising antimicrobial properties. The antimicrobial properties of the phenothiazine derivative improved when the arysulphonyl chloride functionalities were incorporated to the later phenothiazine compound, which is a very important and a new discovery made in this research. Finding new, affordable treatment alternatives is supported by the synthesized compounds encouraging antibacterial properties. When resources are few, their development could help lessen the economic strain brought on by resistant illnesses [53].

Author Contributions

E. L. A. conceptualized, designed and supervised the research work; M. O. U. performed synthesis experiments, collected, and analyzed the data; E. L. A. collected computational data and analyzed the data; E. L. A. and M. O. U. performed the characterization of the compounds; E. L. A. analyzed the data and supervised; P. I. E. and T. O. O. supervised and reviewed the

paper. All authors reviewed the manuscript.

Conflicts of Interest

The authors declare no conflict of interest.

Acknowledgement

Eugene L. Ayuk gratefully acknowledges the assistance of Prof. Comfort Nkamule, Department of Chemistry, Tswane University of Technology in Pretoria, Republic of South Africa for the provision of facilities, laboratory space to carry out the synthesis of compounds and their spectral characterization.

References

1. Onoabedje, E. A., Egu, S. A., Ezeokonkwo, M. A., & Okoro, U. C. (2019). Highlights of molecular structures and applications of phenothiazine & phenoxazine polycycles. Journal of Molecular Structure, 1175, 956-962. 10.1016/j.molstruc.2018.08.064.
2. Sochacka, J., Pacholczyk, M., Jeleń, M., Morak-Młodawska, B., & Pluta, K. (2021). Interaction of new tri-, tetra-, and pentacyclic azaphenothiazine derivatives with calf thymus DNA: Spectroscopic and molecular docking studies. Spectrochimica Acta Part A: Molecular and Biomolecular Spectroscopy, 262, 120105. 10.1016/ j.saa.2021.120105.
3. Revoju, S., Matuhina, A., Canil, L., Salonen, H., Hiltunen, A., Abate, A., & Vivo, P. (2020). Structure-induced optoelectronic properties of phenothiazine-based materials. Journal of Materials Chemistry C, 8(44), 15486-15506. 10.1039/d0tc03421e.
4. Kenia, H., Shivkumar, B., Kotnal, R. B., Ramesha, A., Devadiga, P., Simpi, C. C., & Chandrashekar, V. M. (2020). "Synthesis and Evaluation of Phenothiazine Derivatives". IOSR Journal of Pharmacy, 10, 54-62.
5. Varga, B., Csonka, A., Csonka, A., Molnar, J., Amaral, L., & Spengler, G. (2017). Possible biological and clinical applications of phenothiazines. Anticancer Research, 37(11), 5983-5993. 10.21873/anticanres.12045.
6. Gopi, C., & Dhanaraju, M. D. (2019). Recent progress in synthesis, structure and biological activities of phenothiazine derivatives. Review Journal of Chemistry, 9(2), 95-126. 10.1134/ s2079978019020018.
7. Bazin, I., & Desmarchelier, M. (2022). Retrospective study on the use of fluvoxamine in 72 dogs with anxiety disorders. Journal of Veterinary Behavior, 50, 60-69. 10.1016/ j.jveb.2022.01.001.
8. Cunningham Owens, D., & Johnstone, E. C. (2018). The development of antipsychotic drugs. Brain and Neuroscience Advances, 2, 2398212818817498. 10.1177/2398212818817498.
9. Seeman, M. V. (2021). History of the dopamine hypothesis of antipsychotic action. World Journal of Psychiatry, 11(7), 355-364. 10.5498/wjp.v11.i7.355.
10. Chatterjee, S., & Chatterjee, R. P. (2023). In Cognizance of schizophrenia: A profound insight into the psyche 113-125. 10.1007/978-981-19-7022-1_8.
11. Howland, R. H. (2016). Methylene blue: The long and winding road from stain to brain: Part 2. Journal of Psychosocial Nursing and Mental Health Services, 54(10), 21-26. 10.3928/02793695-20160920-04.
12. Posso, M. C., Domingues, F. C., Ferreira, S., & Silvestre, S. (2022). Development of phenothiazine hybrids with potential medicinal interest: A review. Molecules, 27(1). 10.3390/ molecules27010276.
13. Lavanya, R. (2017). Sulphonamides: A pharmaceutical review. International Journal of Pharmaceutical Science Invention, 6, 1-3.
14. Gulcin, I., & Taslimi, P. (2018). Sulfonamide inhibitors: A patent review 2013–present. Expert Opinion on Therapeutic Patents, 28(7), 541-549. 10.1080/13543776.2018.1487400.
15. Hutchings, M. I., Truman, A. W., & Wilkinson, B. (2019). Antibiotics: Past, present and future. Current Opinion in Microbiology, 51, 72-80. 10.1016/ j.mib.2019.10.008.
16. Al-Mudhafar, M. M. J., Abdulkadir, M. Q., Mohammed, A., Al-hilli, F. A., & Hussian, A. M. (2012). Synthesis and microbiological study of new sulphonamides. International Journal of Comprehensive Pharmacy, 3, 10-13.
17. Buyukkidan, N., Bulbul, M., Kasimogullari, R., & Buyukkidan, B. (2013). Synthesis and characterization of metal complexes of heterocyclic sulfonamide as carbonic anhydrase inhibitors. Journal of Enzyme Inhibition and Medicinal Chemistry, 28(2), 311-315. 10.3109/14756366.2012.712516.
18. Chinchilli, K. K., Angeli, A., Thacker, P. S., Korra, L. N., Biswas, R., Arifuddin, M., & Supuran, C. T. (2020). Design, synthesis, and biological evaluation of 1,2,3-triazole-linked triazino[5,6-b]indole-benzene sulfonamide conjugates as potent carbonic anhydrase I, II, IX, and XIII inhibitors. Metabolites, 10(5). 10.3390/ metabo10050200.
19. El-Qaliei, M. I. H., El-Gaby, M., Ammar, Y. A., Ali, A. M., Hussein, M. F., & Faraghally, F. A. (2020). Sulfonamides: Synthesis and the recent applications in medicinal chemistry. Egyptian Journal of Chemistry. 10.21608/ ejchem.2020.33860.2707.
20. Berdugo, M., Delaunay, K., Naud, M. C., Guegan, J., Moulin, A., Savoldelli, M., …& Behar-Cohen, F. (2021). The antidiabetic drug glibenclamide exerts direct retinal neuroprotection. Translational Research, 229, 83-99. 10.1016/ j.trsl.2020.10.003.
21. Awad, S. H., Sahib, S. A., Hussein, F. A., & Hasan Al-Khfaji, H. A. (2019). Synthesis, characterization and study of biological activity of new para-methoxy benzene sulfonamide derivatives and some amino acid. IOP Conference Series: Materials Science and Engineering, 571(1). 10.1088/1757-899x/571/1/012093.
22. Ghorab, M. M., Soliman, A. M., Alsaid, M. S., & Askar, A. A. (2020). Synthesis, antimicrobial activity and docking study of some novel 4-(4,4-dimethyl-2,6-dioxocyclohexylidene)methylamino derivatives carrying biologically active sulfonamide moiety. Arabian Journal of Chemistry, 13(1), 545-556. 10.1016/j.arabjc.2017.05.022.
23. Clare, B. W., Scozzafava, A., & Supuran, C. T. (2001). Protease inhibitors: Synthesis of a series of bacterial collagenase inhibitors of the sulfonyl amino acyl hydroxamate type. Journal of Medicinal Chemistry, 44(13), 2253-2258. 10.1021/jm010087e.
24. Tačić, A., Nikolić, V., Nikolić, L., & Savić, I. (2017). Antimicrobial sulphonamide drugs. Advanced Technologies, 6, 58-71.
25. Ovung, A., & Bhattacharyya, J. (2021). Sulfonamide drugs: Structure, antibacterial property, toxicity, and biophysical interactions. Biophysical Reviews, 13(2), 259-272. 10.1007/s12551-021-00795-9.

26. Masters, P. A., O'Bryan, T. A., Zurlo, J., Miller, D. Q., & Joshi, N. (2003). Trimethoprim-sulfamethoxazole revisited. Archives of Internal Medicine, 163(4), 402-410. 10.1001/ archinte.163.4.402.
27. Variya, H. H., Panchal, V., & Patel, G. R. (2021). Synthesis, anti-tuberculosis and anti-bacterial activities of sulfonamide bearing 4-((2-(5-bromo-1H-pyrazolo[3,4-b] pyridin-1-yl)-2-oxoethyl)amino)-N-(various substitutions) benzenesulfonamide. Indian Journal of Chemistry – Section B, 59(5). 10.56042/ijcb.v59i05.45469.
28. Liu, J., Seibold, S. A., Rieke, C. J., Song, I., Cukier, R., & Smith, W. L. (2007). Prostaglandin endoperoxide H synthases: Peroxidase hydroperoxide specificity and cyclooxygenase activation. Journal of Biological Chemistry, 282(25), 18233-18244. 10.1074/jbc.M701235200.
29. Rehman, H., Qadir, A., Ali, Z., Nazir, S., Zahra, A., & Shahzady, T. G. (2018). Synthesis and characterization of novel sulfonamides derivatives and their antimicrobial, antioxidant and cytotoxicity evaluation. Bulletin of the Chemical Society of Ethiopia, 31(3). 10.4314/bcse.v31i3.13.
30. Akocak, S., Lolak, N., Bua, S., & Supuran, C. T. (2018). Discovery of novel 1,3-diaryltriazene sulfonamides as carbonic anhydrase I, II, VII, and IX inhibitors. Journal of Enzyme Inhibition and Medicinal Chemistry, 33(1), 1575-1580. 10.1080/14756366.2018.1515933.
31. Hussein, E. M., Al-Rooqi, M. M., Elkhawaga, A. A., & Ahmed, S. A. (2020). Tailoring of novel biologically active molecules based on N-substituted sulfonamides bearing thiazole moiety exhibiting unique multi-addressable biological potentials. Arabian Journal of Chemistry, 13(5), 5345-5362. 10.1016/j.arabjc.2020.03.014.
32. Guzman, J. D. (2014). Natural cinnamic acids, synthetic derivatives and hybrids with antimicrobial activity. Molecules, 19(12), 19292-19349. 10.3390/molecules191219292.
33. Satyanarayana, B., Muralikrishna, P., Kumar, D. R., & Ramachandran, D. (2013). Preparation and biological evaluation of phenothiazine derivatives. Journal of Chemical and Pharmaceutical Research, 5(5), 262-266.
34. Ayuk, E. L., Oforji, C. F., Ugwu, F., Aronimo, S. B., & Njokunwogbu, A. (2017). Determination of secondary metabolites and biological potential of Gnetum africanum (Okazi) leaves. The Pharmaceutical and Chemical Journal, 4(4), 115-122.
35. Song, L., & Ji, Q. (n.d.). The crystal structure of Staphylococcus aureus CntA in apo form. Protein Data Bank. 10.2210/pdb5yh5/pdb.
36. Rodzli, N. A., Kamaruddin, S., Jonet, A., Seman, W. M. K. W., Tab, M. M., Minor, N., …& Illias, R. M. D. (n.d.). Proline iminopeptidase from psychrophilic yeast Glaciozyma antarctica. Protein Data Bank. 10.2210/pdb5yhp/ pdb.
37. Mima, M., & Ushiyama, F. (n.d.). Crystal structure of E. coli DNA gyrase B in complex with 2-oxo-1,2-dihydroquinoline derivative. Protein Data Bank. 10.2210/pdb6kzv/pdb.
38. 38. Bergeron, J. R. C., & Strynadka, N. C. J. (n.d.). Crystal structure of PrgK 19-92. Protein Data Bank. 10.2210/pdb-4w4m/pdb.
39. Wei, W. F., & Van Aalten, D. M. F. (n.d.). Aspergillus fumigatus Rho1 F25N. Protein Data Bank. 10.2210/pdb5zvp/ pdb.
40. Bax, B. D., Chan, P., Eggleston, D. S., Fosberry, A., Gentry, D. R., Gorrec, F., …& Gwynn, M. N. (n.d.). The twinned 3.35 Å structure of S. aureus gyrase complex with ciprofloxacin and DNA. Protein Data Bank. 10.2210/pdb2xct/ pdb.
41. Rodriguez-Almazan, C., Arreola-Alemon, R., Rodriguez-Larrea, D., Aguirre-Lopez, B., de Gomez-Puyou, M. T., Perez-Montfort, R., & Costas, M. (n.d.). Structural basis of human triosephosphate isomerase deficiency. Mutation E104D and correlation to solvent perturbation. Protein Data Bank. 10.2210/pdb2vom/pdb.
42. Daina, A., Michielin, O., & Zoete, V. (2017). SwissADME: A free web tool to evaluate pharmacokinetics, drug-likeness and medicinal chemistry friendliness of small molecules. Scientific Reports, 7, 42717. 10.1038/srep42717.
43. Lipinski, C. A., Lombardo, F., Dominy, B. W., & Feeney, P. J. (1997). Experimental and computational approaches to estimate solubility and permeability in drug discovery and development settings. Advanced Drug Delivery Reviews, 23(1-3), 3-25. 10.1016/s0169-409x(96)00423-1.
44. Ayuk, E. L., Okoro, U. C., Ibeji, C. U., & Nkambule, C. M. (2023). Synthesis, in silico studies and investigations on antimicrobial, antimalarial activities of p-toluenesulphonamoyl 'Leu-Gly' dipeptide carboxamide derivatives. Journal of Molecular Structure, 1285. 10.1016/ j.molstruc.2023.135529.
45. Lipinski, C. A. (2004). Lead- and drug-like compounds: The rule-of-five revolution. Drug Discovery Today: Technologies, 1(4), 337-341. 10.1016/ j.ddtec.2004.11.007.
46. Omran, Z., & Rauch, C. (2014). Acid-mediated Lipinski's second rule: Application to drug design and targeting in cancer. European Biophysics Journal, 43(4-5), 199-206. 10.1007/s00249-014-0953-1.
47. Veber, D. F., Johnson, S. R., Cheng, H. Y., Smith, B. R., Ward, K. W., & Kopple, K. D. (2002). Molecular properties that influence the oral bioavailability of drug candidates. Journal of Medicinal Chemistry, 45(12), 2615-2623. 10.1021/ jm020017n.
48. Chapman, K. L., Holzgrefe, H., Black, L. E., Brown, M., Chellman, G., Copeman, C., …& Wilson, S. (2013). Pharmaceutical toxicology: Designing studies to reduce animal use, while maximizing human translation. Regulatory Toxicology and Pharmacology, 66(1), 88-103. 10.1016/j. yrtph.2013.03.001.
49. Bennion, B. J., Be, N. A., McNerney, M. W., Lao, V., Carlson, E. M., Valdez, C. A., …& Carpenter, T. S. (2017). Predicting a drug's membrane permeability: A computational model validated with in vitro permeability assay data. The Journal of Physical Chemistry B, 121(20), 5228-5237. 10.1021/acs.jpcb.7b02914.
50. Ertl, P., Rohde, B., & Selzer, P. (2000). Fast calculation of molecular polar surface area as a sum of fragment-based contributions and its application to the prediction of drug transport properties. Journal of Medicinal Chemistry, 43(20), 3714-3717. 10.1021/ jm000942e.
51. Prasanna, S., & Doerksen, R. J. (2009). Topological polar surface area: A useful descriptor in 2D-QSAR. Current Medicinal Chemistry, 16(1), 21-41. 10.2174/092986709787002817.
52. Daga, P. R., Bolger, M. B., Haworth, I. S., Clark, R. D., & Martin, E. J. (2018). Physiologically based pharmacokinetic modeling in lead optimization. 2. Rational bioavailability design by global sensitivity analysis to identify properties affecting bioavailability. Molecular Pharmaceutics, 15(3),

831-839. 10.1021/ acs.molpharmaceut.7b00973.
53. Doak, B. C., Over, B., Giordanetto, F., & Kihlberg, J. (2014). Oral druggable space beyond the rule of 5: Insights from drugs and clinical candidates. Chemistry & Biology, 21(9), 1115-1142. 10.1016/j.chembiol.2014.08.013.